OXFORD

Carcinogenesis, 2018, Vol. 39, No. 2, 202–213

doi:10.1093/carcin/bgx124
Advance Access publication November 2, 2017
Original Article

ORIGINAL ARTICLE

Induction of non-apoptotic programmed cell death by oncogenic RAS in human epithelial cells and its suppression by MYC overexpression

Kasumi Dendo[1,2], Takashi Yugawa[1], Tomomi Nakahara[1], Shin-ichi Ohno[1], Naoki Goshima[3], Hirofumi Arakawa[2,4] and Tohru Kiyono[1,*]

[1]Division of Carcinogenesis and Cancer Prevention, National Cancer Center Research Institute, 5-1-1 Tsukiji, Chuo-ku, Tokyo 10-40045, Japan, [2]Department of NCC Cancer Science, Graduate School of Medical and Dental Sciences, Tokyo Medical and Dental University, 1-5-45 Yushima, Bunkyou-ku, Tokyo 113–8510, Japan, [3]Molecular Profiling Research Center for Drug Discovery, National Institute of Advanced Industrial Science and Technology, 2-4-7 Aomi, Koto-ku, Tokyo, 135-0064, Japan and [4]Division of Cancer Biology, National Cancer Center Research Institute, 5-1-1 Tsukiji, Chuo-ku, Tokyo 104-0045, Japan

*To whom correspondence should be addressed. Tel: +81 3 3547 5275; Fax: +81 3 3543 2181; Email: tkiyono@ncc.go.jp

Abstract

Oncogenic mutations of RAS genes, found in about 30% of human cancers, are considered to play important roles in cancer development. However, oncogenic RAS can also induce senescence in mouse and human normal fibroblasts. In some cell lines, oncogenic RAS has been reported to induce non-apoptotic programed cell death (PCD). Here, we investigated effects of oncogenic RAS expression in several types of normal human epithelial cells. Oncogenic RAS but not wild-type RAS stimulated macropinocytosis with accumulation of large-phase lucent vacuoles in the cytoplasm, subsequently leading to cell death which was indistinguishable from a recently proposed new type of PCD, methuosis. A RAC1 inhibitor suppressed accumulation of macropinosomes and overexpression of MYC attenuated oncogenic RAS-induced such accumulation, cell cycle arrest and cell death. MYC suppression or rapamycin treatment in some cancer cell lines harbouring oncogenic mutations in RAS genes induced cell death with accumulation of macropinosomes. These results suggest that this type of non-apoptotic PCD is a tumour-suppressing mechanism acting against oncogenic RAS mutations in normal human epithelial cells, which can be overcome by MYC overexpression, raising the possibility that its induction might be a novel approach to treatment of RAS-mutated human cancers.

Introduction

The RAS family genes HRAS, KRAS and NRAS, which encode small GTPases, constitute one of the most common groups of oncogenes mutated in human cancers. Approximately, 30% of cancers harbour activating mutations. However, there are currently no available molecular target drugs specific for activated RAS. Interestingly, mutation rates in cancers can be drastically different depending on the tissue or cell type (1). For instance, KRAS is found to be mutated in more than 90% of pancreatic cancers and in this case, is thought to be an initial driver mutation, whereas RAS mutations occur only very rarely in stomach and breast cancers.

Normal cells have evolved multiple antitumour responses to prevent aberrant growth. Oncogenic RAS is known to induce senescence or cell death depending on the cell type. Senescence induced by oncogenes such as RAS genes is known as oncogene-induced cellular senescence, as well documented in normal human and mouse fibroblasts (2–5). Oncogenic RAS is also reported to induce a caspase-independent cell death in neuroblastoma (6) and a non-apoptotic programmed cell death (PCD) associated with accumulation of macropinosomes in glioblastoma cell lines (7–10), respectively, indicating that RAS-responsive safeguard mechanisms are conserved even in some

Received: December 30, 2016; **Revised:** October 13, 2017; **Accepted:** October 27, 2017

Abbreviations

4-OHT	4-hydroxytamoxifen
DOX	doxycycline
hTERT	human telomerase reverse transcriptase
PCD	programmed cell death
TMR	tetramethylrhodamine

transformed cells. However, in normal human epithelial cells, detailed mechanisms regarding antitumour responses to oncogenic RAS are not fully understood.

Macropinocytosis is a type of endocytosis, which is a feature of most eukaryotic cells and mostly involves fluid and solutes. Macropinosomes are heterogenous vesicles, which vary in size from 0.2–10 μm in diameter. Macropinocytosis occurs spontaneously and is enhanced upon virus infection or in response to growth factors which activate receptor tyrosine kinases and induce the actin-mediated membrane ruffling (11–15). Constitutive macropinocytosis occurs in fibroblasts transformed with oncogenic v-Src or Kras (16,17). RAS activation of RAC1 is known to result in membrane ruffling (18,19). It was reported that in pancreatic cancer cells with RAS mutations, macropinocytosis also occurs and supplies extracellular proteins which are degraded into amino acids in lysosomes and then enter carbon metabolism (20). However, in other cancer cell lines, exogenous expression of oncogenic mutant RAS was reported to induce macropinocytic cell death (8–10). Such differences might be attributable to cell-type dependence or variation in expression levels of RAS.

In the present study, we aimed to elucidate molecular mechanisms underlying oncogenic RAS-driven cell death and also its suppression in RAS-induced carcinogenesis. Upon induction of oncogenic RAS in several types of normal human epithelial cells, accumulation of large vacuoles in the cytoplasm, macropinosomes, was observed and the affected cells ceased to proliferate. Moreover, accumulation of macropinosomes was suppressed when MYC was overexpressed. These results indicate that this type of PCD functions as an antitumour response against oncogenic mutation of RAS genes, which is conserved among normal human epithelial cells. Our findings also suggest that MYC overexpression, which is frequently observed in many cancers, can override such an antitumour response to oncogenic RAS, and this may to some extent account for the strong cooperation between RAS and MYC in cancer development.

Materials and methods

Cell culture

Normal human cells were obtained with written consent from patients under approval of the Ethical Committee at each Hospital. The study protocol was approved by National Cancer Center Institutional Review Board. Normal human cervical keratinocytes, HCK1, were obtained who underwent abdominal surgery for a gynecological disease other than cervical cancer. The HCK1T cell line was established by transduction of the catalytic subunit of human telomerase reverse transcriptase (hTERT: T) into HCK1 (21) and maintained in serum-free keratinocyte-SF medium (Invitrogen, Life Technologies, Saint Aubin, France) supplemented with 5 ng/ml human epidermal growth factor (E9644; Sigma-Aldrich, St. Louis, MO, USA) and 50 μg/ml of bovine pituitary extract (Hammond Cell Tech, San Francisco, CA, USA). The cervical cancer cell lines, HeLa (a gift from Dr. M. Inagaki, Aichi Cancer Center, Japan, JCRB9004, ICRB Cell Bank in 1996, authenticated by short tandem repeat analysis, expression of HPV18 E7 was confirmed by immunoblotting in 2009) and OMC4, the lung cancer cell line, A549 (authenticated by short tandem repeat analysis in 2017), and the pancreatic cancer cell line, AsPC-1 (purchased from ATCC, Manassas, VA, USA), were maintained in F-medium at least for 2 weeks before the assays. F-medium is composed of Dulbecco's modified Eagle's medium :F12 (1:3 mixture) supplemented with 0.4 μg/ml hydrocortisone (H-4001; Sigma-Aldrich), 30 μg/ml adenine hydrochloride (016-00802; Wako Pure Chemical Industries, Ltd), 8.4 ng/ml cholera toxin (C8052; Sigma-Aldrich), 5 μg/ml insulin (090-03441; Wako Pure Chemical Industries, Ltd) and 5% fetal bovine serum (172012; Sigma-Aldrich). The following drugs were used: 4-hydroxytamoxifen (4-OHT) (T176; Sigma-Aldrich), doxycycline (DOX) (63131; Clontech, Mountain View, CA, USA), rapamycin (R-5000; Funakoshi Co., Ltd, Tokyo, Japan) and EHT1864 (3872; Tocris Bioscience, Minneapolis, MN, USA).

Retroviral vector construction and transduction

Retroviral vector plasmids were constructed by using the Gateway system according to the manufacturer's instructions (Invitrogen, Life Technologies). Human $KRAS^{G12V}$ (22), fused to the ligand binding domain of murine oestrogen receptor, mER^{T2}, derived from LZRS ERTmRasV12 (23), a gift from P. Khavari (Addgene plasmid # 21199), was cloned into the entry vector to make pENTR221-mER^{T2}-$KRAS^{G12V}$. Wild-type version of mER^{T2}-KRAS was generated by *in vitro* mutagenesis. These were recombined into retroviral expression vectors to generate pCLXIN-mER^{T2}-$KRAS^{G12V}$, -KRAS, pQCXIP-mER^{T2}-$KRAS^{G12V}$ and -KRAS. Construction of pCMSCVpuro-MYC was described previously (21). pENTR201-$RAC1^{Q61L}$ was generated from pENTR201-RAC (HGPD, FLJ30431AAAN) by *in vitro* mutagenesis. $HRAS^{G12V}$, $RAC1^{Q61L}$ and EGFP-OmoMYC (24) were recombined with a lentiviral vector, CSII-TRE-Tight-RfA (22), to generate CSII-TRE-Tight-$HRAS^{G12V}$, -$RAC1^{Q61L}$ and -EGFP-OmoMYC. A KRAS-specific short hairpin RNA expression vector, pSI-MSCVpuro-H1R-shKRAS, was generated as described previously (25) except for 5′-CAGTTGAGACCTTCTAATTGG-3′ (26) was chosen as the targeted sequence. The production of recombinant retroviruses and lentiviruses and selection of infected cells were as detailed earlier (27,28). Lentiviruses without drug selection markers were inoculated at a multiplicity of infection of more than five.

Immunoblotting

Whole-cell protein extracts were used for analysis, and immunoblotting was conducted as described previously (21). Primary antibodies against pan-RAS (C-4) (sc-166691; Santa Cruz Biotechnology, Santa Cruz, CA, USA), KRAS (sc30; Santa Cruz), RAC1 (05-389; Merck-Millipore, Billerica, MA, USA), MYC-tag (9E10.2) (supernatant of hybridoma), GFP (A6455; Invitrogen, Life Technologies) and vinculin (V9264; Sigma-Aldrich) were used as probes. Horseradish peroxidase-conjugated antimouse and antirabbit (Jackson ImmunoResearch Laboratories, West Grove, PA, USA) immunoglobulins were used as the secondary antibodies. The LAS3000 CCD-Imaging System (Fujifilm Co. Ltd, Tokyo) was employed for detection of proteins visualized by Lumi-light plus Western blotting substrate (Roche).

Dextran incorporation assay

Four and seven days after adding indicated concentrations of 4-OHT and DOX, respectively, cells were incubated with 0.4 mg/ml dextran-Alexa Fluor 488 (D22910; Invitrogen, Life Technologies) or 0.4 mg/ml dextran-tetramethylrhodamine (TMR) (D1818; Invitrogen, Life Technologies) for 3 h and washed with phosphate-buffered saline. The nuclei were stained with Hoechst 33342 (H-1399; Life Technologies) for 30 min. Images of the cells were acquired by ArrayScan VTI System, and dextran-fluorescence signals within the areas surrounding counterstained nuclei were quantified using Cellomics Scan Software (Thermo Fisher Scientific K.K., Hudson, NH, USA). About up to 1000 cells per well of quadruplicate wells were analysed per each sample. Signal intensity of 10 000 with 7.4 ms exposure was set as 1 so as to indicate relative intensity per cell.

RAC1 activation assay

Activated RAC1 was collected using a Rac1 Pull-down Activation Assay Biochem Kit (Cytoskeleton Inc., Denver, CO, USA) according to the manufacturer's instructions. Assays were conducted on cells harvested on the 4th–7th days after the addition of 4-OHT or DOX. Active RAC1, as well as total RAC1, was quantified by immunoblotting using anti-RAC1 antibody.

Results

Activated RAS-induced cell death is accompanied by enhanced vacuolation

We reported previously that expression of activated RAS (RAS^{G12V}) and MYC together with HPV16 E6E7 (E6E7) is enough to transform several types of normal human epithelial cells from various organs such as cervix, pancreas, ovary and tongue (21,22,29,30). When only activated RAS was overexpressed in these epithelial cells, we noticed massive cell death with accumulation of many vacuoles in the cytoplasm. In order to characterize the phenotype triggered by expression of activated RAS in detail, we generated HCK1T, normal human cervical keratinocytes immortalized by hTERT (21), expressing mER^{T2}-$KRAS^{G12V}$ (ER-$KRAS^{G12V}$) chimeric protein whose functions could be regulated by 4-OHT (23). After 4-OHT was added to the media, ER-$KRAS^{G12V}$ protein was gradually accumulated. The accumulated levels of ER-$KRAS^{G12V}$ protein were comparable with endogenous RAS at day 2 (Figure 1A), when vacuoles in the cytoplasm and a flattened morphology became evident (Figure 1B). The majority of the cells were vacuolated and flattened at day 4 (Figure 1B) while the levels of ER-$KRAS^{G12V}$ at day 4 was still less than that of endogenous wild-type KRAS overexpressed in the cervical cancer cell line, OMC4 (Figure 1A). When cells were exposed different concentrations of 4-OHT, accumulation of ER-$KRAS^{G12V}$ proteins and vacuolation of cells were induced in a dose-dependent manner (Supplementary Figure 1A, available at *Carcinogenesis* Online). Next, the wild-type KRAS-fusion protein,

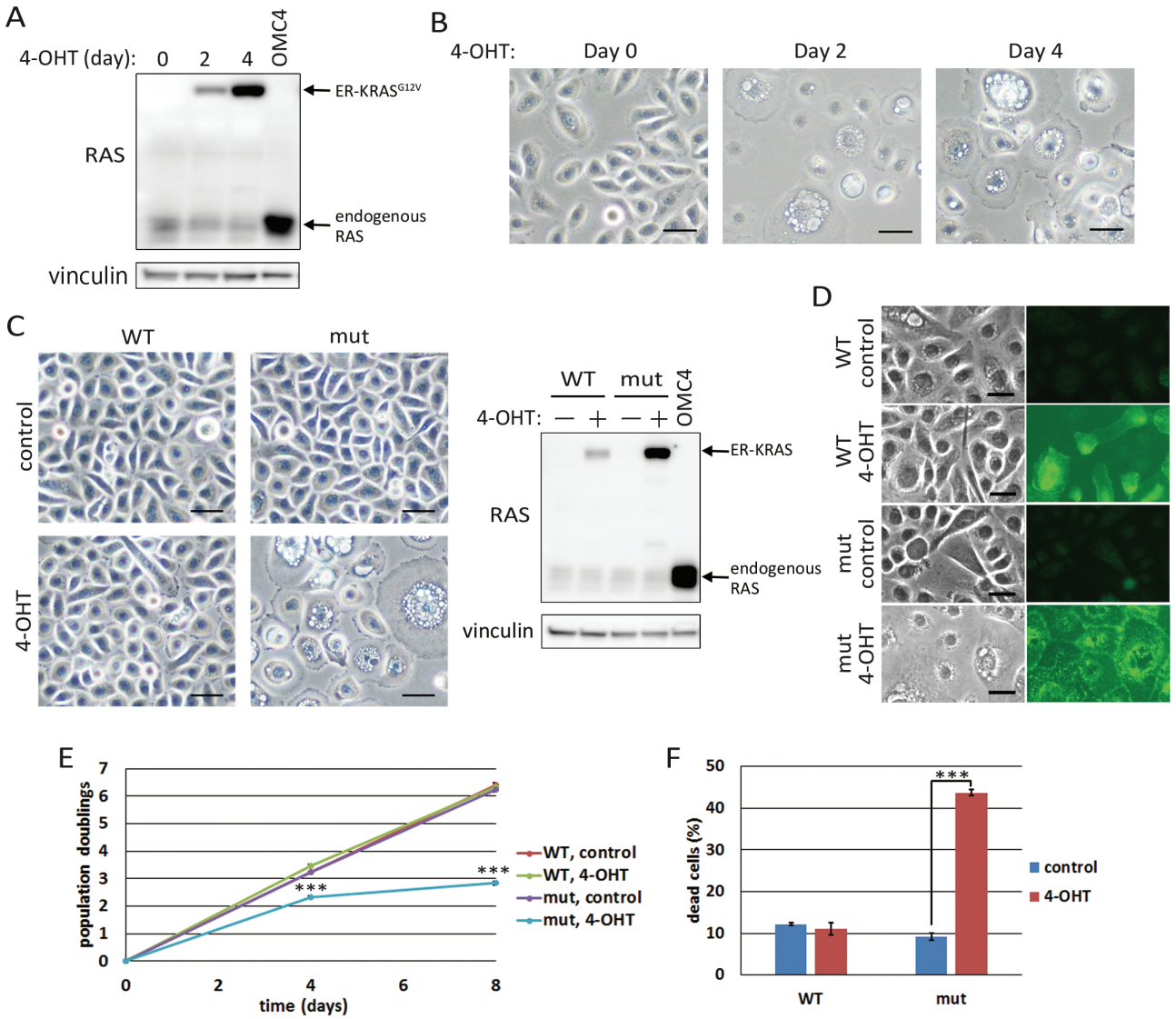

Figure 1. Oncogenic RAS induces vacuolation leading to cell death in normal human epithelial cells. (**A**) HCK1T/mER^{T2}-$KRAS^{G12V}$ (HCK1T/ER-$KRAS^{G12V}$) cells were treated with 100 nM 4-OHT for 2 or 4 days. Expression of RAS proteins and vinculin as a loading control were detected by Western blotting. OMC4, cervical cancer cell line, expressing a high level of wild-type KRAS was included as a control. (**B**) After treatment as for (A), induction of vacuolation was detected by phase-contract microscopy. Scale bars represent 50 μm. (**C**) HCK1T/ER-$KRAS^{G12V}$ (mut) and /ER-KRAS (WT) cells were treated with 100 nM 4-OHT or vehicle (control) for 4 days. Representative images of the cells by phase-contract microscopy are shown (left). Scale bars represent 50 μm. Expression of RAS proteins and vinculin were detected by Western blotting (right). (**D**) Immuno-fluorescent staining of RAS proteins in HCK1T/ER-$KRAS^{G12V}$ and /ER-KRAS cells on 4th day after addition of 100 nM 4-OHT. Scale bars represent 25 μm. (**E**) Growth curves of HCK1T/ER-$KRAS^{G12V}$ and /ER-KRAS cells. Each point is the mean of triplicate values ± standard deviation. ***$P \leq 0.001$ according to Student's *t* test. (**F**) HCK1T/ER-$KRAS^{G12V}$ and /ER-KRAS cells were treated with 100 nM 4-OHT for 4 days, and trypan blue positive cells were counted. Each bar represents the mean of the triplicate values ± standard deviation. ***$P \leq 0.001$ according to Student's *t* test.

mER^{T2}-KRAS (ER-KRAS), was expressed in the cells under control of the same long terminal repeat (LTR) promoter used for ER-KRAS^{G12V} expression. Accumulation of the protein was less and no morphological changes were observed (Figure 1C). To examine whether the vacuolation is induced specifically by the mutant RAS, the wild-type ER-KRAS was additionally expressed under the control of cytomegalovirus immediate early (CMV IE) promoter in the same cells. Though the levels of ER-KRAS protein far exceeded those of ER-KRAS^{G12V} proteins, only weak induction of small vacuoles in some cells was observed (Supplementary Figure 1B, available at *Carcinogenesis* Online). Furthermore, little vacuolation was observed in cells expressing the ER-KRAS$^{G12V/T144E/T148E}$ mutant that should degrade faster than the wild-type, and indeed, there was scarce accumulation upon 4-OHT treatment, whereas strong vacuolation was observed in cells expressing the ER-KRAS$^{G12V/T144A/T148A}$ mutant, which should be more stable than the wild-type (31) (Supplementary Figure 2, available at *Carcinogenesis* Online). RAS proteins clearly accumulated on the surfaces of vacuoles as well as the plasma membranes in activated RAS-expressing cells while they were found mainly perinuclear cytoplasm as well as on the plasma membranes in wild-type RAS-expressing cells (Figure 1D). These results indicate that accumulation of a certain amount of active guanosine triphosphate (GTP)-bound] form of KRAS is required for induction of phenotypes, including vacuolation and flattened morphology.

We also generated DOX-inducible HRAS^{G12V}-expressing HCK1T by transducing LXIN-rtTA (tetON) and CSII-TRE-Tight-HRAS^{G12V}, HCK1T/ON/HRAS^{G12V} cells, and obtained essentially the same results upon DOX treatment (Supplementary Figure 1C, available at *Carcinogenesis* Online). Furthermore, we also applied the 4-OHT-inducible or DOX-inducible system to other normal human epithelial cells, and induction of vacuolation was commonly observed in examples isolated from the pancreatic duct, ovary, tongue, dermis, bladder, oesophagus, mammary gland and prostate upon induction of activated RAS proteins (Supplementary Figure 1D, available at *Carcinogenesis* Online). Of note, these vacuolated cells were also enlarged and flattened, with mean diameters more than twice those of non-vacuolated cells. So, hereafter, we just focused on HCK1T to examine molecular mechanisms underlying this phenotype.

Cells expressing ER-KRAS^{G12V} showed reduced proliferation upon treatment of 4-OHT, and scarcely propagated after passage, while wild-type ER-KRAS-expressing cells as well as parental HCK1T proliferated exponentially at similar rates (Figure 1E). Trypan blue staining of the cells indicated increased cell death upon treatment of 4-OHT in ER-KRAS^{G12V}-expressing cells but not in ER-KRAS-expressing cells (Figure 1F). These results suggested that accumulation of activated KRAS induced vacuolation and subsequent cell death.

Activated RAS-induced vacuoles are originated from macropinosomes

In glioblastoma cell lines, it is reported that activated HRAS induces cell death through hyperstimulation of micropinocytosis (8–10). The authors proposed naming the new type of cell death, methuosis, derived from the Greek word 'methuo', which means to drink to intoxication (9). In order to investigate whether activated RAS-induced vacuoles were formed by macropinocytosis, incorporation of fluorescence-labelled dextran with a molecular weight larger than 70 kDa (dextran-TMR) was examined. Activated RAS-expressing cells incorporated much more dextran-TMR compared with control or wild-type RAS-expressing cells (Figure 2A). Moreover, vacuoles were filled with dextran in activated RAS-expressing cells (Figure 2B). Time-lapse photography indicated that smaller vacuoles were initially formed by uptake of extracellular fluid and then fused to become larger vacuoles, which was consistent with the process forming macropinosomes (Figure 2C and Supplementary Figure 3, available at *Carcinogenesis* Online). Together, these data indicated that the vacuolation induced by activated RAS was caused by enhanced macropinocytosis, with accumulation of excessively uptaken extracellular fluids into the cells subsequently leading to cell death.

RAS-induced macropinocytosis occurs through RAC1 signalling

RAC1 is known to be a downstream target of RAS and a major factor leading to micropinocytosis (18,19). As methuosis in glioblastoma cells was reported to be caused through RAC1 activation (10), we tested whether RAC1 is involved in RAS-induced macropinocytosis in HCK1T. Total amounts of RAC1 as well as the activated form increased following accumulation of ER-KRAS^{G12V} proteins (Figure 3A and Supplementary Figure 1A, available at *Carcinogenesis* Online). Moreover, suppression of RAC1 activity with EHT1864 repressed RAS-induced vacuolation (Figure 3B). Of note, EHT1864 suppressed vacuolation but not enlargement or flattening of HCK1T/ER-KRAS^{G12V} cells upon 4-OHT treatment, indicating that two pathways are in parallel control under RAS signalling, one inducing macropinocytosis, the other causing enlargement and flattening, which are reminiscent of senescent phenotypes.

Next, to examine whether activated RAC1 alone could induce cell death as in activated RAS-expressing cells, we generated HCK1T conditionally expressing activated RAC1 (RAC1^{Q61L}), HCK1T/OFF/RAC1^{Q61L} cells, in which RAC1^{Q61L} was repressed in the presence of DOX. Six days after removal of DOX, vacuolation of cells was evident. However, enlargement and flattening were less apparent compared with the case with activated RAS-expressing cells (Figure 3C). Dextran incorporation into vacuoles was also confirmed (Figure 3D). Decreased proliferation and increased death were also observed in activated RAC1-expressing cells (Figure 3E and F). In these cells expressing activated RAS or RAC1, no signs of apoptosis, such as rounding of cell shape, nuclear condensation and fragmentation, were noted. Effects of downstream targets of RAS other than RAC1 were also examined by transducing constitutively active forms of AKT (myr-AKT) or MEK1/2 (MEK1/2-DD). However, neither induced vacuolation nor flattening of cells (data not shown). The results demonstrated that activated RAS induces excess macropinocytosis and cell death mainly through RAC1 activation in human normal epithelial cells, which coincides with the proposed features of a new type of PCD, methuosis (9,10).

Inhibition of RAS-induced cell death by MYC overexpression

Since we described previously that co-expression of activated RAS, MYC and E6E7 in several epithelial cells, including HCK1, is sufficient to induce tumorigenic transformation (21,22), the combination of MYC and E6E7 could suppress cell death induced by activated RAS. We also noticed expression of E6E7 alone did not suppress RAS-induced vacuolation (Supplementary Figure 4, available at *Carcinogenesis* Online). Others also reported that activated RAS can induce non-apoptotic cell death, which they call autophagic cell death though, in human ovarian surface epithelial cell (HOSE) immortalized by E6E7 and hTERT (32). Thus,

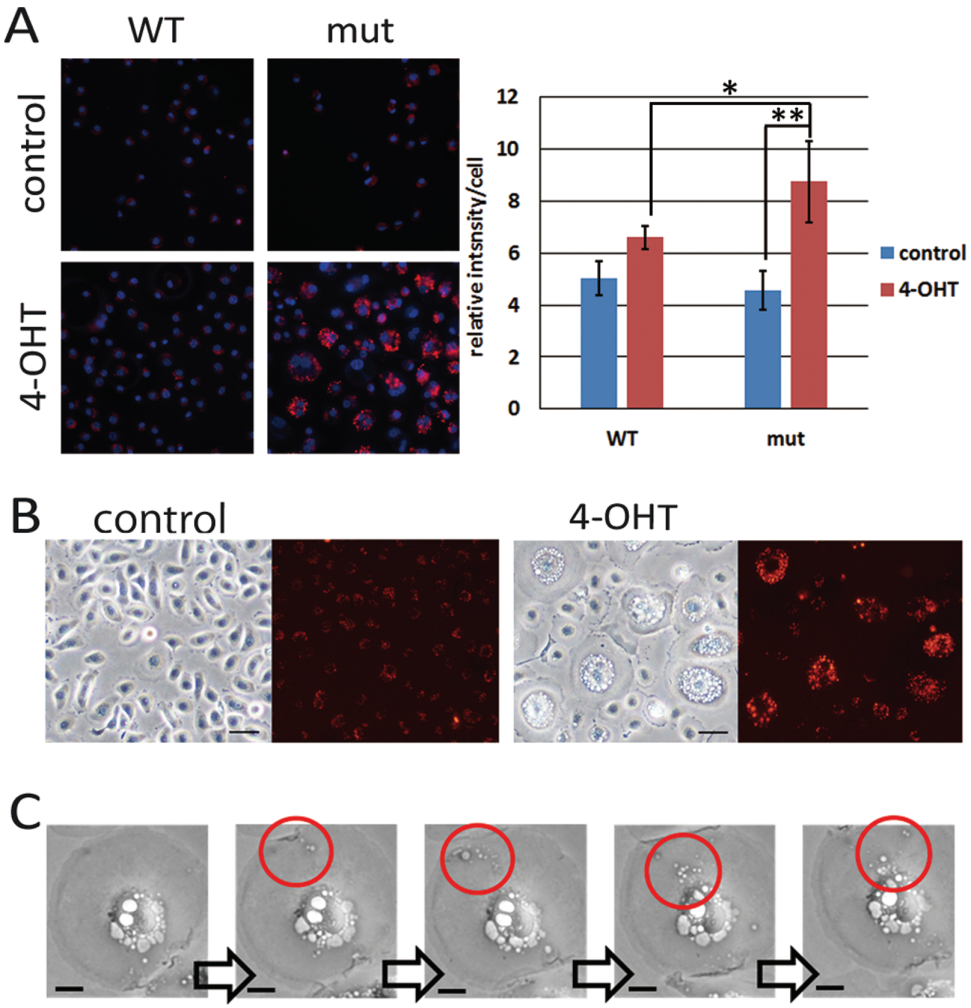

Figure 2. RAS-induced vacuolation is caused by hyperstimulation of macropinocytosis. (**A**) HCK1T/ER-KRAS^{G12V} (mut) and /ER-KRAS (WT) cells were treated with 100 nM 4-OHT or vehicle (control). On the 4th day, cells were incubated in the presence of dextran-TMR for 3 h and stained with Hoechst 33342 (left). The intensity of dextran was quantified (right). Each bar represents the mean of intensity values ± standard deviation (n = 4). *P ≤ 0.05 and **P ≤ 0.01 according to Student's t test. (**B**) Cells were treated with 100 nM 4-OHT. Next day, cells were incubated in the presence of dextran-TMR for 3 h and washed. Representative phase-contrast and fluorescent images on the 4th day are shown. Note that most vacuoles were filled with dextran in 4-OHT treated cells. Scale bars represent 50 μm. (**C**) HCK1T/ON/HRAS^{G12V} cells were treated with 1 μg/ml DOX and analysed by a time-lapse photography. Photos taken every 30 min from 42 to 44 h after adding DOX are shown. Macropinosomes incorporated from cell surface moving into perinuclear region are shown in red circles. Scale bars represent 2.5 μm.

we focused on MYC as a candidate suppressor of RAS-induced cell death (Figure 4A) and transduced wild-type MYC or empty vector into HCK1T/ER-KRAS^{G12V} cells. While many vacuoles in the cytoplasm were observed in vector-transduced cells upon 4-OHT treatment, they were rare in MYC-overexpressing cells (Figure 4B). The intensity of dextran incorporation was reduced in MYC-expressing cells compared with the case of vector cells upon 4-OHT treatment (Figure 4C). Interestingly, the intensity of incorporated dextran was lower in MYC-overexpressing cells even in the absence of 4-OHT, suggesting that MYC can regulate accumulation of macropinosomes even in normal epithelial cells. In accordance with these observations, suppression of cell proliferation and elevated cell death upon treatment of 4-OHT were also alleviated by co-expression of MYC (Figure 4D and E), though MYC-expressing cells showed slightly higher levels of dead cells compared with vector-control cells in the absence of 4-OHT, perhaps due to MYC-induced apoptosis (33).

Next, we tested whether MYC can suppress macropinocytosis by activated RAC1. We transduced wild-type MYC or an empty vector into HCK1T/OFF/RAC1^{Q61L} cells. Upon RAC1^{Q61L} expression on DOX withdrawal, vacuolation was induced in the vector-transduced cells but rarely in MYC-co-expressing cells (Figure 4F), which was confirmed by dextran incorporation assays (Figure 4G). Interestingly, accumulation of ER-KRAS^{G12V} and activated RAC1 proteins was also inhibited in MYC-co-expressing cells (Figure 4B and F). Since KRAS proteins were mainly localized on the surfaces of vacuoles (Figure 1D), it seems likely that vacuolation further increases the accumulation of KRAS and possibly RAC1 proteins, though we could not examine the localization of RAC1 due to a lack of a specific antibody with high sensitivity. Taken together, the results indicate that overexpression of MYC can alleviate both activated RAS- and RAC1-induced cell death through inhibition of macropinosome accumulation.

MYC suppression and rapamycin treatment reactivate PCD in an in vitro carcinogenesis model

We showed previously that transduction of oncogenic RAS and E6E7 can confer tumorigenicity on normal human cervical keratinocyte (HCK), and additional transduction of MYC strongly

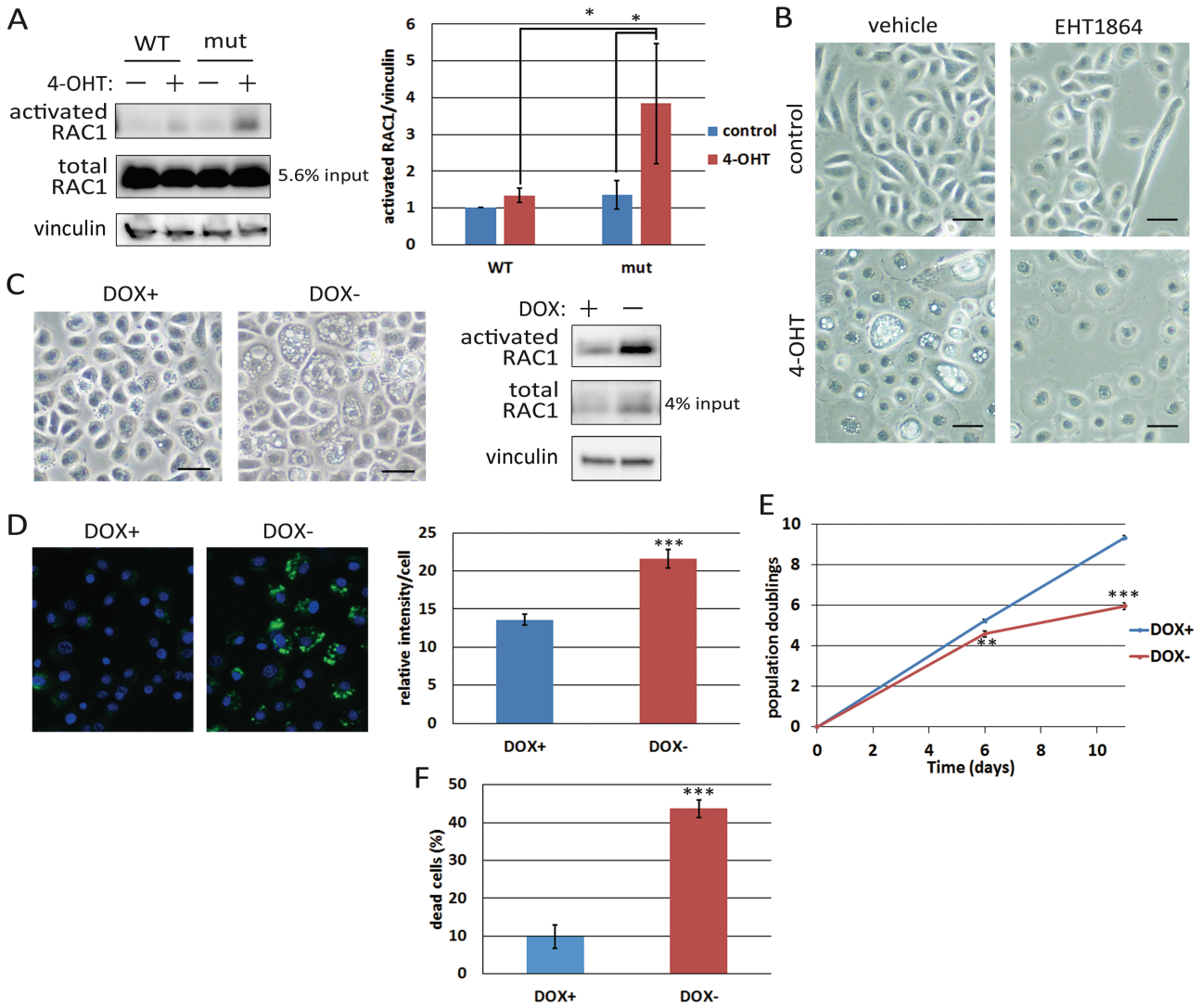

Figure 3. RAS-induced cell death is elicited through the RAS-RAC1 pathway. (**A**) HCK1T/ER-KRAS^{G12V} (mut) and /ER-KRAS (WT) cells were treated with 100 nM 4-OHT or vehicle (–) for 4 days. Activated RAC1 levels were determined by pull down assays as described in Materials and methods. Expression levels of total RAC1 as well as vinculin were also determined by Western blotting. Pull down assays were performed three times, and a representative result is shown (left). The activated RAC1 level of control cells with WT KRAS was set at one. The activated RAC levels were quantified (right). Each bar represents the mean of ratios ± standard deviation. (**B**) HCK1T/ER-KARS^{G12V} cells were pretreated with 5 μM EHT1864, a RAC1 inhibitor, or vehicle for 2 h before adding 100 nM 4-OHT or vehicle and incubated for 2 days. Representative phase-contrast images are shown. Scale bars represent 50 μm. (**C**) HCK1T/OFF/RAC1^{Q61L} cells maintained in the presence of 1 μg/ml DOX were incubated for 6 days in the presence (+) or absence (–) of DOX. Representative images were taken by a phase-contrast microscope (left), and activated RAC1 levels were determined by the pull down assay as in (A) (right). Scale bars represent 50 μm. (**D**) HCK1T/OFF/RAC1^{Q61L} cells were treated as in (C). Seven days after DOX withdrawal, cells were incubated in the presence of dextran-Alexa488 for 3 h, and stained with Hoechst 33342. Fluorescent images of the cells were taken (left) and the intensity of the incorporated dextran was quantified (right). Each bar represents the mean of intensity values ± standard deviation (n = 4). (**E**) Growth curves of HCK1T/OFF/RAC1^{Q61L} cells in the continued presence of DOX (+) or after withdrawal of DOX (–). Each point is the mean of triplicate values ± standard deviation. (**F**) HCK1T/OFF/RAC1^{Q61L} cells were treated as in (E). Trypan blue positive cells were counted at day 11. Each bar represents the mean of triplicate values ± standard deviation. $^{*}P \leq 0.05$, $^{**}P \leq 0.01$ and $^{***}P \leq 0.001$ according to Student's t test.

enhanced the tumorigenic potential, while additional transduction of OmoMYC, which binds to MAX and act as a dominant negative MYC (24,34,35), or rapamycin treatment strongly attenuated tumour formation (21,27). Thus, we wondered whether MYC suppression and/or rapamycin might inhibit tumorigenic potential through induction of oncogenic RAS-driven cell death. To examine this possibility, we transduced DOX-regulatable E6E7 and MYC into HCK1T/ER-KRAS^{G12V} cells (HCK1T/ER-KRAS^{G12V}/OFF/E6E7-MYC: HCK1T/EMR), in which E6E7 and MYC were expressed in the absence of DOX (Supplementary Figure 5A, available at *Carcinogenesis* Online). These cells demonstrated tumorigenic potential when all the four oncogenes were activated or expressed (data not shown), and macropinosomes accumulated when the expression of E6E7 and MYC was shut-off by DOX administration (Supplementary Figure 6A, upper middle, available at *Carcinogenesis* Online). Interestingly, ER-KRAS^{G12V} protein was decreased when MYC and E6E7 were co-expressed (4-OHT+, DOX–) as in HCK1T/ER-KRAS^{G12V}/MYC cells (Figure 4B and Supplementary Figure 5B, available at *Carcinogenesis* Online).

To examine how MYC suppresses RAS-induced macropinosome accumulation, we exposed HCK1T/EMR cells to dextran in a condition expressing activated RAS, E6E7 and MYC (4-OHT+, DOX–), and then the amount of remaining dextran in the cells treated with or without DOX was chased. Levels in

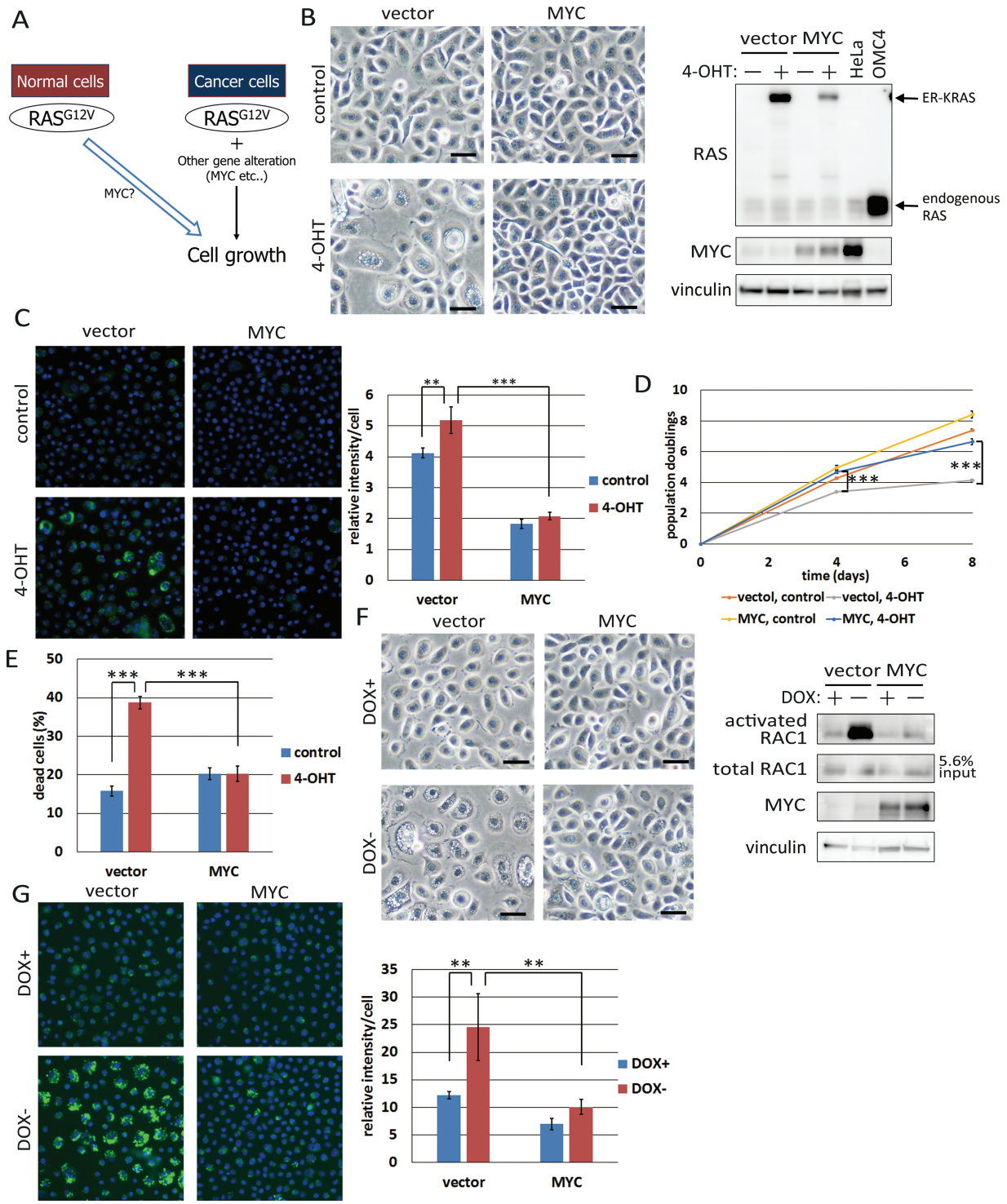

Figure 4. Overexpression of MYC suppresses RAS-induced cell death. (**A**) Graphical summary of the experiments in this figure. (**B**) HCK1T/ER-KRAS^{G12V} cells transduced with MYC (HCK1T/ER-KRAS^{G12V}/MYC) or vector (HCK1T/ER-KRAS^{G12V}/vector) were treated with 10 nM 4-OHT or vehicle for 4 days. Representative phase-contrast images are shown (left), and expression levels of RAS and MYC as well as vinculin were determined by Western blotting (right). OMC4 and HeLa, cervical cancer cell lines, were included as controls. Scale bars represent 50 μm. (**C**) HCK1T/ER-KRAS^{G12V}/MYC or /vector cells were treated with dextran-Alexa488 and stained with Hoechst 33342 on the 4th day after treatment as in (B). Fluorescent images were taken (left), and the intensities of dextran-AlexaA488 were quantified (right). Each bar represents the mean of relative intensity values ± standard deviation ($n = 4$). (**D**) Growth curves of HCK1T/ER-KRAS^{G12V}/MYC and /vector cells. Cells were incubated as in (B) and the cells were counted on the 4th and 8th days. Each point is the mean of triplicate values ± standard deviation. (**E**) Cells were treated as in (B), and trypan blue positive cells were counted at day 4. Each bar represents the mean of triplicate values ± standard deviation. (**F**) HCK1T/OFF/RAC1^{Q61L} cells transduced with MYC or vector were maintained in the presence of 1 μg/ml DOX. Cells were incubated in the presence or absence of DOX for 6 days. Representative phase-contrast images were shown (left). Scale bars represent 50 μm. Activated RAC1 levels determined by pull down assay and total RAC1 and MYC as well as vinculin levels determined by western blotting are shown (right). (**G**) Cells were treated as in (**F**) for 7 days. On the 7th day, cells were incubated with dextran-Alexa488 for 3 h and stained with Hoechst 33342. Representative fluorescent images are shown (left), and the fluorescent intensities of dextran-AlexaA488 were quantified (right). Each bar represents the mean of intensity values ± standard deviation ($n = 4$). $^{**}P \leq 0.01$ and $^{***}P \leq 0.001$ according to Student's *t* test.

cells expressing only activated RAS (4-OHT+, DOX+) were higher than in those continuously expressing activated RAS and E6E7-MYC (4-OHT+, DOX–), suggesting that MYC at least in the presence of E6E7 had the ability to enhance recycling pathways (Supplementary Figure 5C, available at *Carcinogenesis* Online). In agreement with this, ER-KRAS^{G12V} protein gradually accumulated by shutting off E6E7 and MYC expression (DOX administration) (Supplementary Figure 5B, available at *Carcinogenesis* Online).

Next, we treated activated RAS-expressing HCK1T with 100 nM rapamycin. Vacuolation with dextran uptake was markedly enhanced, whereas no increase was observed in cells without activated RAS expression (Figure 5A and B). Accumulation of macropinosomes was also observed in the cells expressing activated RAS, E6E7 and MYC (4-OHT+, DOX–) but not in cells without expression of all four genes (4OHT–, DOX+) upon treatment with rapamycin (Supplementary Figure 6, available at *Carcinogenesis* Online).

PCD can be induced by MYC suppression and rapamycin treatment in cancer cells harbouring RAS mutations

Given that activated mutations in RAS genes could induce PCD in normal epithelial cells also *in vivo* (36), the process should be suppressed in cancer cells harbouring activated mutations of RAS genes. Since deregulated expression of MYC is frequently observed in many cancers (37,38), and overexpression of MYC can suppress PCD induced by activated RAS in HCK1T, we examined whether suppression of endogenous MYC function by OmoMYC could induce PCD in cancer cell lines harbouring RAS mutations. We fused OmoMYC with green fluorescent protein (GFP) protein to monitor expression of OmoMYC by DOX addition (24) (Figure 6A and Supplementary Figure 7A and B, available at *Carcinogenesis* Online). The GFP-OmoMYC expression level was several times higher than that of endogenous MYC (Figure 6B and Supplementary Figure 7C, available at *Carcinogenesis* Online). Growth inhibition and cell death were induced not only in A549 and AsPC-1 cells, lung and pancreatic cancer cell lines, respectively, harbouring RAS mutations, but also in HeLa cells, a cervical cancer cell line, harbouring wild-type RAS (Figure 6C and D and Supplementary Figure 7D and E, available at *Carcinogenesis* Online). However, cytoplasmic large vacuoles were induced only in A549 and AsPC-1 cells but not in HeLa cells (Figure 6A and Supplementary Figure 7A and B, available at *Carcinogenesis* Online). In fact, incorporation of dextran-TMR was observed in large vacuoles in A549 cells. In HeLa cells, dextran accumulation was also induced by MYC inhibition, but dextran was observed only in small vesicles which could hardly identified in the bright field images (Figure 6E and F and Supplementary Figure 7F and G, available at *Carcinogenesis* Online). It seems likely that non-fused small macropinosomes were accumulated in HeLa cells possibly through enhanced recycling of macropinosomes by MYC (Supplementary Figure 5C, available at *Carcinogenesis* Online). Thus, cell death observed in HeLa cells depends on a mechanism other than macripinocytic cell death. We also attempted to suppress MYC by three miRs. Formation of large vacuoles with dextran incorporation and cell death in A549 cells were significantly

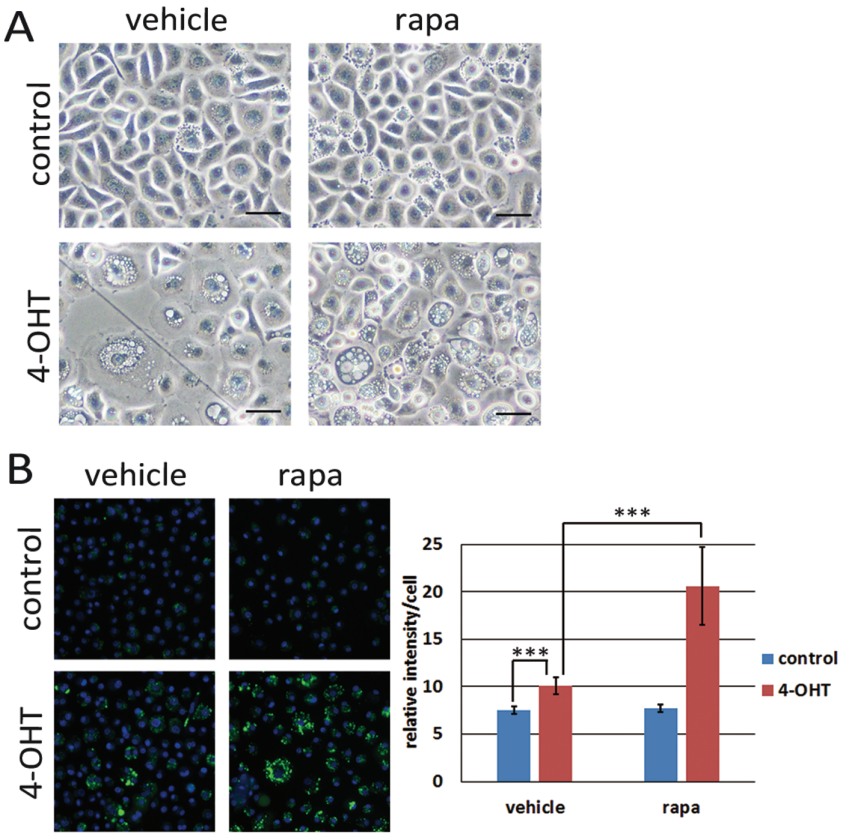

Figure 5. Accumulation of macropinosomes is enhanced by rapamycin. (**A**) HCK1T/ER-KRAS^{G12V} cells were treated with 100 nM 4-OHT or vehicle (control) and 100 nM rapamycin (rapa) or vehicle for 3 days. Representative phase-contrast images are shown. Scale bars represent 50 μm. (**B**) HCK1T/ER-KRAS^{G12V} cells were treated as in (A). On the 2nd day, cells were incubated in the presence of dextran-Alexa488 for 3 h, stained with Hoechst 33342, and the fluorescent images were taken (left), and the intensities of dextran-Alexa488 were quantified (right). Each bar indicates mean intensity ± standard deviation ($n = 4$). ***$P \leq 0.01$ according to Student's *t* test.

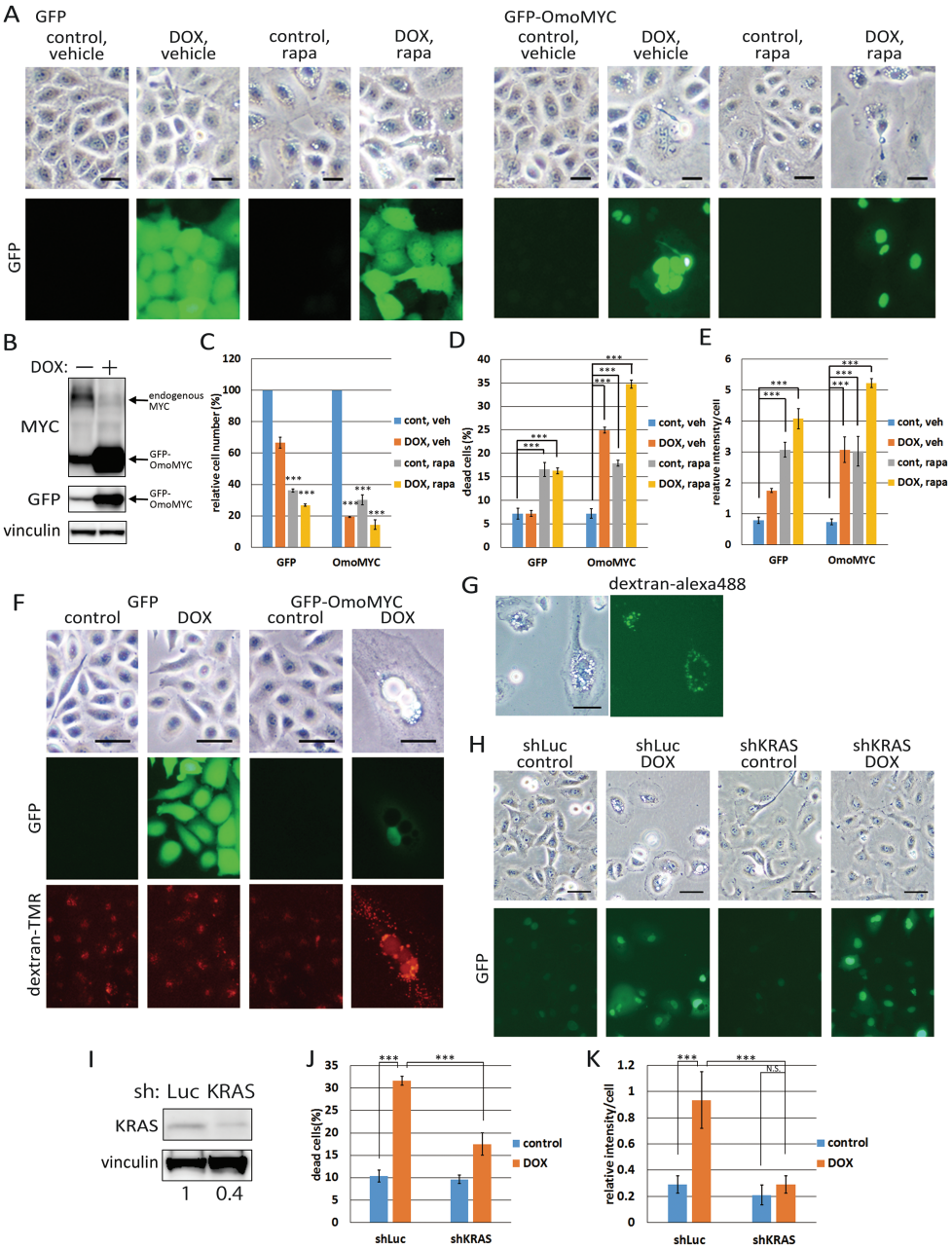

Figure 6. Accumulation of macropinosomes is enhanced by MYC suppression or rapamycin treatment in A549 cancer cell line harbouring RAS mutation. (**A**) A549 cells were first transduced with LXIN-tetON to generate A549/ON cells. These cells were then transduced with CSII-TRE-Tight-GFP-OmoMYC and CSII-TRE-Tight-GFP to generate A549/ON/GFP-OmoMYC and A549/ON/GFP cells, respectively. Cells were treated with 100 nM rapamycin (rapa) or vehicle for 4 days in the presence or absence of 1 μg/ml DOX. Representative phase-contrast and GFP-fluorescent images are shown. Scale bars represent 25 μm. (**B**) A549/ON/GFP-OmoMYC and /GFP cells were incubated in the presence or absence of 1 μg/ml DOX for 4 days, and the expression levels of GFP-OmoMYC as well as endogenous MYC were determined by Western blotting with anti-MYC antibody. GFP and GFP-OmoMYC proteins were also detected by anti-GFP antibody. Vinculin was detected as a control. (**C**) The relative cell numbers on the 4th day after treated as in (A) were indicated by setting the number of control cells (DOX–/rapa–) to 100. Each bar represents the mean of triplicate values ± standard deviation. (**D**) Cells treated as in (A) for 4 days were stained with trypan blue. Percentages of trypan blue positive cells were indicated. Each bar represents the mean of triplicate values ± standard deviation. (**E**) A549 cells were pre-incubated with dextran-TMR for 24 h and washed. Then the cells were similarly treated as in (A) for 4 days, stained with 4′,6-diamidino-2-phenylindole. Dextran-TMR intensity was quantified. Each bar represents the mean of triplicate values ± standard deviation. (**F**) A549/ON/GFP-OmoMYC or /GFP cells were incubated in the presence or absence of 1 μg/ml DOX. Next day, cells were incubated in the presence of dextran-TMR for 3 h and washed. Representative phase-contrast and fluorescent images of TMR and GFP on the 4th day are shown. Note that most large vacuoles were filled with TMR in DOX-treated A549/ON/GFP-OmoMYC cells. Scale bars represent 50 μm. (**G**) After A549/ON/GFP-OmoMYC, cells were treated with 100 nM rapamycin for 4 days, cells were incubated in the presence of dextran-Alexa488 for 3 h. Representative phase-contrast and fluorescent images are shown. Scale bars represent 50 μm. (**H**) A549/ON/GFP-OmoMYC cells were transduced with MSCVpuro-H1R-sh-KRAS or -sh-luciferase. Cells were incubated in the presence or absence of DOX for 4 days. Representative phase-contrast and GFP-fluorescent images are shown. Scale bars represent 50 μm. (**I**) Levels of endogenous KRAS as well as vinculin were determined by Western blotting. The intensity of KRAS normalized by vinculin in the control cells was set at one and the relative intensities were indicated at the bottom. (**J**) Trypan blue positive cells treated as in (H) were counted at day 4. Each bar represents the mean of triplicate values ± standard deviation. (**K**) A549/ON/GFP-OmoMYC/shKRAS and /sh-luciferase cells were pre-incubated with dextran-TMR for 24 h and washed. Then, the cells were similarly treated as in (H) for 4 days, stained with 4′,6-diamidino-2-phenylindole and fluorescent images were taken. Dextran-TMR intensities were quantified. Each bar represents the mean of intensity values ± standard deviation ($n = 4$). ***$P \leq 0.001$ according to Student's t test.

induced by one miR (miR2), which strongly silenced MYC, followed by miR3 but rarely induced by the other miR (miR1) and control miR (GFPmiR), further supporting that MYC suppression induced non-apoptotic PCD in A549 cells (Supplementary Figure 8, available at *Carcinogenesis* Online).

Next, we also examined the possibility that rapamycin can enhance accumulation of macropinosomes in cancer cell lines harbouring RAS mutations (Figure 6A and Supplementary Figure 7A and B, available at *Carcinogenesis* Online). Increased accumulation of incorporated dextran was observed only in A549 and AsPC-1 cells though decreased proliferation and increase of dead cells were observed for all cell lines in the presence of rapamycin (Figure 6C-E and Supplementary Figure 7D, E and G, available at *Carcinogenesis* Online). Vacuoles were filled with dextran in rapamycin-treated A549 cells (Figure 6G). Moreover, dextran incorporation in other non-RAS mutated cancer cell lines, H520 and BxPC-3, appeared to be unaffected upon treatment of rapamycin (Supplementary Figure 9, available at *Carcinogenesis* Online).

Finally, to examine whether cell death induced by MYC suppression depends on oncogenic RAS, we knocked down mutant KRAS in the OmoMYC-expressing A549 cells. KRAS silencing significantly attenuated OmoMYC-induced vacuolation, dextran accumulation and cell death to the levels almost equivalent to those of control cells (Figure 6H-K), strongly indicating that the cell death induced by MYC suppression depends on mutant KRAS expressed in A549 cells.

Taken together, these results indicate that OmoMYC and rapamycin facilitate accumulation of macropinosomes in some cancer cells with RAS mutations, which might be one of the mechanisms whereby MYC inhibition and rapamycin can induce growth inhibition and cell death at least partly through processes related to 'methuosis'.

Discussion

The results of the present study indicate that overexpression of oncogenic RAS induces non-apoptotic PCD in normal human epithelial cells, mainly through RAC1 activation. Oncogene-induced cellular senescence is considered to be a tumour suppressor mechanism. However, it has been studied mainly using fibroblasts and only rarely in epithelial cells. We propose that PCD is a tumour suppressor mechanism against oncogenic RAS-induced epithelial carcinogenesis. However, since only about 30% of human cancers harbour oncogenic mutations of RAS genes, we must consider the possibility that other alterations might also impact this tumour suppressor pathway. Oncogenic RAS-induced cell death in HCK1T was not suppressed by co-expression of E6E7 but rather by overexpression of MYC (Figure 4 and Supplementary Figure 4, available at *Carcinogenesis* Online). We reported previously that expression levels of MYC are critical for transformation of human cells by E6E7 and oncogenic HRAS (27), and the combination of E6E7, oncogenic RAS and MYC was sufficient for tumorigenic transformation of normal human epithelial cells from cervix, tongue and pancreas (21,22,30). Others reported that high expression of oncogenic RAS was required for tumorigenic transformation of normal human mammary epithelial cells in the presence of co-expressed SV40 LT and hTERT genes, and the resultant tumorigenic cells harboured amplification of the MYC gene (39). The present study provided clues to a mechanism underlying why expression levels of MYC are critical in transformation of normal human epithelial cells by E6E7 and oncogenic RAS.

One might argue that oncogenic RAS-induced cell death requires very high levels of oncogenic RAS. Indeed, cancers arise from many organs with activation of oncogenic Kras gene alone in transgenic mouse models (40,41). However, only a small fraction of cells with oncogenic Ras can develop cancer, and some organs are almost completely resistant to oncogenic Ras-induced cancer development in a mouse model (36). In humans, more than 95% of pancreatic ductal adenocarcinomas harbour oncogenic KRAS mutations, while few mutations in RAS genes are found in gastric and breast cancers. Thus, it is possible that RAS-induced PCD functions more efficiently in these latter as a tumour suppressor mechanism to eliminate RAS-mutated cells also *in vivo*, though clearly further studies are required to provide support for this conclusion.

Very recently, it was reported that Kras copy gains are positively selected during progression of lung cancer in a Kras transgenic mouse model, and amplification of a mutant RAS allele is also frequently found in human cancers, associated with a more aggressive phenotype (42). Amplification and deregulated expression of MYC are also frequently found in human cancers, linked with tumour aggression and a poor clinical outcome (37,38). Therefore, in RAS-driven cancers, increased expression of MYC might allow higher expression of oncogenic RAS. Vice versa, since wild-type RAS is reported to suppress MYC-induced apoptosis (43), overexpression of oncogenic RAS then might allow higher expression of MYC. MYC induces apoptosis mainly through p53 activation (44), and HPV16 E6, which can target p53 for degradation (45), can suppress MYC-induced apoptosis. Indeed, a combination of MYC and E6E7 can more strongly suppress the oncogenic RAS-induced cell death than MYC alone (Figure 4 and Supplementary Figure 5 and 6, available at *Carcinogenesis* Online). Interconnected co-operation of the oncogenes might thus explain the highly tumorigenic potential observed in normal human epithelial cells transduced with a combination of oncogenic RAS, MYC and E6E7 (21,22,30). Consistent with our results obtained by *in vitro* study, there is a tendency towards co-occurrence of MYC overexpression and oncogenic mutations of KRAS gene in The Cancer Genome Atlas (TCGA) datasets of a large fraction of human lung adenocarcinomas (230 patients, TCGA, Nature 2014) (46) and lung squamous cell carcinomas (178 patients, TCGA, Nature 2012) (47), suggesting the co-operation of these two oncogenes in cancer development.

We reported previously that MYC inhibition by expression of OmoMYC or administration of rapamycin strongly suppressed tumorigenic potential of HCK1T transformed with E6E7 and oncogenic RAS (27). In the present study, we obtained evidence that RAS-induced PCD is at least one of the mechanisms involved in such tumour suppression. The results allow us to consider the possibility that inhibition of MYC by expression of OmoMYC and rapamycin administration might induce PCD in established cancer cell lines harbouring mutations in RAS genes. We could provide evidence that accumulation of macropinosomes is induced by OmoMYC or rapamycin in A549 and AsPC-1 cells harbouring RAS mutations, but not in HeLa, H520 and BxPC-3 cells harbouring wild-type RAS genes (Figure 6 and Supplementary Figure 7 and 9, available at *Carcinogenesis* Online). EGFR-RAS signalling abnormalities are found in the majority of cancers. Though receptor tyrosine kinase inhibitors have been developed and are in successful clinical use, no drugs are clinically available specifically targeting oncogenic RAS proteins. Here, we present evidence that MYC inhibition and rapamycin administration might be useful to kill RAS-mutated cancer cells by enhancing non-apoptotic PCD, based on a tumour suppressor

function conserved in normal human epithelial cells. Merits of this strategy include increased incorporation and longer intracellular retention of large sized particles such as drug-encapsulated micelles into RAS-mutated cancer cells. Clearly, further studies are required to elucidate molecular mechanisms of RAS-induced PCD in normal epithelial cells and its suppression in RAS-driven cancer cells. Most important is the proof of concept that RAS-driven cancer cells might be specifically treated by induction of PCD.

In pancreatic adenocarcinoma cells, oncogenic RAS is reported to enhance macropinocytosis to support increased cell metabolism, and pharmacological inhibition of macropinocytosis was found to compromise the growth of RAS-transformed pancreatic tumour xenografts (20). Thus, increased uptake of extracellular nutrition by macropinocytosis seems generally present in RAS-driven tumour cells. Therefore, it is reasonable to conclude that cells with increased macropinosomes due to oncogenic RAS expression cannot be processed properly like normal epithelial cells leading to PCD, and that MYC overexpression enhances processing of macropinosomes to support increased cell metabolism. Indeed, we obtained evidence that overexpression of MYC inhibited oncogenic RAS-induced cell death at least partially through increased recycling of macropinosomes (Supplementary Figure 5C, available at *Carcinogenesis* Online). At present, we do not know precisely how OmoMYC and rapamycin can induce cell death in RAS-driven tumour cells. Since MYC is reported to be a global amplifier of transcription (48), and rapamycin is an mTORC1 inhibitor which globally suppresses translation, expression of many genes could be influenced by OmoMYC and rapamycin. Rapamycin generally inhibits tumour growth through inhibiting protein synthesis, although recently it was reported that inhibition of mTORC1 by rapamycin or Torin 1 rather increases cell proliferation under conditions of amino acid starvation (49). Thus, it will be important to identify downstream genes and proteins responsible for enhanced recycling of increased macropinosomes, to provide more specific targets to induce cell death in RAS-driven cancers.

Supplementary material

Supplementary data are available at *Carcinogenesis* online.

Funding

This work was supported by National Cancer Center Research and Development Fund (23-B-1 to T.K., 23-A-38 to T.K.); Princess Takamatsu Cancer Research Fund (10-24206 to T.K.); Scientific Research from the Ministry of Education, Culture, Sports, Science, and Technology of Japan (16H04701 to T.K.).

Acknowledgements

We thank Dr. H. Miyoshi and Dr. P. Kavari for plasmid constructs; Dr. H. Nishimura, Dr. K. Aoki, Dr. M. Inagaki, Dr. J. Yokota and Dr. T. Kohno for cell lines; Dr. K. Masutomi, Dr. M. Enari and Dr. T. Ohta for helpful discussion and Dr. N. Egawa, Dr. Y. Inagawa, T. Ishiyama, K. Tanaka, C. Kohno, A. Noguchi, E. Kabasawa and Y. Gotoh for expert technical assistance.
Conflict of Interest Statement: S. O. is an employee of BML, Inc.

References

1. Fernández-Medarde, A. *et al.* (2011) Ras in cancer and developmental diseases. Genes Cancer, 2, 344–358.
2. Serrano, M. *et al.* (1997) Oncogenic ras provokes premature cell senescence associated with accumulation of p53 and p16INK4a. Cell, 88, 593–602.
3. Bartkova, J. *et al.* (2006) Oncogene-induced senescence is part of the tumorigenesis barrier imposed by DNA damage checkpoints. Nature, 444, 633–637.
4. Campisi, J. *et al.* (2007) Cellular senescence: when bad things happen to good cells. Nat. Rev. Mol. Cell Biol., 8, 729–740.
5. d'Adda di Fagagna, F. (2008) Living on a break: cellular senescence as a DNA-damage response. Nat. Rev. Cancer, 8, 512–22.
6. Kitanaka, C. *et al.* (2002) Increased Ras expression and caspase-independent neuroblastoma cell death: possible mechanism of spontaneous neuroblastoma regression. J. Natl. Cancer Inst., 94, 358–368.
7. Chi, S. *et al.* (1999) Oncogenic Ras triggers cell suicide through the activation of a caspase-independent cell death program in human cancer cells. Oncogene. 18: 2281-2290.
8. Kaul, A. *et al.* (2007) Activated Ras induces cytoplasmic vacuolation and non-apoptotic death in glioblastoma cells via novel effector pathways. Cell. Signal., 19, 1034–1043.
9. Overmeyer, J.H. *et al.* (2008) Active ras triggers death in glioblastoma cells through hyperstimulation of macropinocytosis. Mol. Cancer Res., 6, 965–977.
10. Bhanot, H. *et al.* (2010) Induction of nonapoptotic cell death by activated Ras requires inverse regulation of Rac1 and Arf6. Mol. Cancer Res., 8, 1358–1374.
11. Swanson, J.A. (2008) Shaping cups into phagosomes and macropinosomes. Nat. Rev. Mol. Cell Biol., 9, 639–649.
12. Mercer, J. *et al.* (2009) Virus entry by macropinocytosis. Nat. Cell Biol., 11, 510–520.
13. Bohdanowicz, M. *et al.* (2013) Role of phospholipids in endocytosis, phagocytosis, and macropinocytosis. Physiol. Rev., 93, 69–106.
14. Maekawa, M. *et al.* (2014) Sequential breakdown of 3-phosphorylated phosphoinositides is essential for the completion of macropinocytosis. Proc. Natl. Acad. Sci. USA, 111, E978–E987.
15. Egami, Y. *et al.* (2014) Small GTPases and phosphoinositides in the regulatory mechanisms of macropinosome formation and maturation. Front. Physiol., 5, 374.
16. Bar-Sagi, D. *et al.* (1986) Induction of membrane ruffling and fluid-phase pinocytosis in quiescent fibroblasts by ras proteins. Science, 233, 1061–1068.
17. Veithen, A. *et al.* (1996) v-Src induces constitutive macropinocytosis in rat fibroblasts. J. Cell Sci., 109, 2005–2012.
18. Tang, Y. *et al.* (1999) Signals from the Ras, Rac, and Rho GTPases converge on the Pak protein kinase in Rat-1 fibroblasts. Mol. Cell. Biol., 19, 1881–1891.
19. Amyere, M. *et al.* (2000) Constitutive macropinocytosis in oncogene-transformed fibroblasts depends on sequential permanent activation of phosphoinositide 3-kinase and phospholipase C. Mol. Biol. Cell, 11, 3453–3467.
20. Commisso, C. *et al.* (2013) Macropinocytosis of protein is an amino acid supply route in Ras-transformed cells. Nature, 497, 633–637.
21. Narisawa-Saito, M. *et al.* (2008) An *in vitro* multistep carcinogenesis model for human cervical cancer. Cancer Res., 68, 5699–5705.
22. Inagawa, Y. *et al.* (2014) A human cancer xenograft model utilizing normal pancreatic duct epithelial cells conditionally transformed with defined oncogenes. Carcinogenesis, 35, 1840–1846.
23. Dajee, M. *et al.* (2002) Epidermal Ras blockade demonstrates spatially localized Ras promotion of proliferation and inhibition of differentiation. Oncogene, 21, 1527–1538.
24. Annibali, D. *et al.* (2014) Myc inhibition is effective against glioma and reveals a role for Myc in proficient mitosis. Nat. Commun., 5, 4632.
25. Haga, K. *et al.* (2007) Efficient immortalization of primary human cells by p16INK4a-specific short hairpin RNA or Bmi-1, combined with introduction of hTERT. Cancer Sci., 98, 147–154.
26. Singh, A. *et al.* (2009) A gene expression signature associated with "K-Ras addiction" reveals regulators of EMT and tumor cell survival. Cancer Cell, 15, 489–500.
27. Narisawa-Saito, M. *et al.* (2012) A critical role of MYC for transformation of human cells by HPV16 E6E7 and oncogenic HRAS. Carcinogenesis, 33, 910–917.

28. Yugawa, T. *et al.* (2010) DeltaNp63alpha repression of the Notch1 gene supports the proliferative capacity of normal human keratinocytes and cervical cancer cells. Cancer Res., 70, 4034–4044.
29. Sasaki, R. *et al.* (2009) Oncogenic transformation of human ovarian surface epithelial cells with defined cellular oncogenes. Carcinogenesis, 30, 423–431.
30. Zushi, Y. *et al.* (2011) An *in vitro* multistep carcinogenesis model for both HPV-positive and -negative human oral squamous cell carcinomas. Am. J. Cancer Res., 1, 869–881.
31. Wang, M.T. *et al.* (2015) K-Ras promotes tumorigenicity through suppression of non-canonical Wnt signaling. Cell, 163, 1237–1251.
32. Elgendy, M. *et al.* (2011) Oncogenic Ras-induced expression of Noxa and Beclin-1 promotes autophagic cell death and limits clonogenic survival. Mol. Cell, 42, 23–35.
33. Sakamuro, D. *et al.* (1995) c-Myc induces apoptosis in epithelial cells by both p53-dependent and p53-independent mechanisms. Oncogene, 11, 2411–2418.
34. Soucek, L. *et al.* (1998) Design and properties of a Myc derivative that efficiently homodimerizes. Oncogene, 17, 2463–2472.
35. Soucek, L. *et al.* (2002) Omomyc, a potential Myc dominant negative, enhances Myc-induced apoptosis. Cancer Res., 62, 3507–3510.
36. Ray, K.C. *et al.* (2011) Epithelial tissues have varying degrees of susceptibility to KrasG12D-initiated tumorigenesis in a mouse model. PLoS One, 6.
37. Nesbit, C.E. *et al.* (1999) MYC oncogenes and human neoplastic disease. Oncogene, 18, 3004–3016.
38. Beroukhim, R. *et al.* (2010) The landscape of somatic copy-number alteration across human cancers. Nature, 463, 899–905.
39. Elenbaas, B. *et al.* (2001) Human breast cancer cells generated by oncogenic transformation of primary mammary epithelial cells. Genes Dev., 15, 50–65.
40. Jackson, E.L. *et al.* (2001) Analysis of lung tumor initiation and progression using conditional expression of oncogenic K-ras. Genes Dev., 15, 3243–3248.
41. Hingorani, S.R. *et al.* (2003) Preinvasive and invasive ductal pancreatic cancer and its early detection in the mouse. Cancer Cell, 4, 437–450.
42. Kerr, E.M. *et al.* (2016) Mutant Kras copy number defines metabolic reprogramming and therapeutic susceptibilities. Nature, 531, 110–113.
43. Kauffmann-Zeh, A. *et al.* (1997) Suppression of c-Myc-induced apoptosis by Ras signalling through PI(3)K and PKB. Nature, 385, 544–548.
44. Hermeking, H. *et al.* (1994) Mediation of c-Myc-induced apoptosis by p53. Science, 265, 2091–2093.
45. Scheffner, M. *et al.* (1990) The E6 oncoprotein encoded by human papillomavirus types 16 and 18 promotes the degradation of p53. Cell, 63, 1129–1136.
46. Cancer Genome Atlas Research Network. (2014) Comprehensive molecular profiling of lung adenocarcinoma. Nature, 511, 543–50.
47. Cancer Genome Atlas Research Network. (2012) Comprehensive genomic characterization of squamous cell lung cancers. Nature, 489, 519–25.
48. Lin, C.Y. *et al.* (2012) Transcriptional amplification in tumor cells with elevated c-Myc. Cell, 151, 56–67.
49. Palm, W. *et al.* (2015) The utilization of extracellular proteins as nutrients is suppressed by mTORC1. Cell, 162, 259–270.